

RESEARCH

Open Access



# Design methodology of standing-wave thermoacoustic refrigerator: theoretical analysis

Mohanad Q. Kamil, Samir Gh. Yahya and Itimad D. J. Azzawi\*

## Abstract

Thermoacoustic refrigeration systems are one of the best alternative solutions for conventional refrigeration systems that are harmful to the environment and humans due to global warming and ozone layer depletion issues. Thermoacoustic technology can be considered a renewable and clean technology with a promising future for its many advantages. A thermoacoustic refrigerator converts acoustic energy to thermal energy (creating a cooling effect). In the present research, the focus is on the design of a standing-wave thermoacoustic refrigerator driven by an ordinary loudspeaker using the numerical simulation program DELTAEC with the concern of building the apparatus at a low cost. In addition, investigating the influence of some crucial parameters on cooling power and thermal/overall performance. Hence, the designed thermoacoustic refrigerator performed well in respect of cooling power and coefficient of performance. It has achieved a cooling power of 134.34 W with a temperature difference between the ambient and cold heat exchangers of 25 K at a COP of 1.956 and the overall efficiency (electrical power converted into cooling power) amounted to 113.43%. The achieved cooling power and COP could be significant when compared to others' results.

**Keywords** DELTAEC, Thermoacoustics, Standing-wave, Refrigerator, Renewable energy, COP

## 1 Introduction

Conventional refrigeration technology (e.g., absorption and vapor compression refrigeration systems) is still dominating and becoming increasingly important in many different fields, including industrial, medicinal, gas liquefaction, missiles, ships, and other vital aspects of daily life. Most conventional refrigeration systems use CFCs (chlorofluorocarbons) which are extremely harmful to the ozone layer and can cause global warming issues. On the other hand, thermoacoustic refrigeration systems are considered to be a new green technology (with no impact on the environment) and can be a good alternative to conventional refrigeration systems [1–3]. Thermoacoustic refrigeration is distinguished from other

refrigeration techniques by the absence of moving parts (no lubrication is required), the ease with which it can be manufactured using locally available materials at a low cost, and, most importantly, the fact that it uses air or inert gases (such as helium) as a working gas, which makes it environmentally friendly. Another advantage of this technology over conventional refrigeration systems is the ability to use a proportional control system for loudspeaker operation based on the cooling load to save electricity (part load operation) [4, 5]. It should be pointed out that the coefficient of performance (COP) of thermoacoustic refrigeration systems is relatively low when compared to conventional refrigeration systems. Improving the COP of thermoacoustic refrigeration systems is an important challenge in developing these systems to commercially compete with the rest of conventional refrigeration systems.

Thermoacoustics is a scientific term that describes how the two major areas of thermodynamics and acoustics interact. In other words, thermal (heat) power can be

\*Correspondence:

Itimad D. J. Azzawi

Itimaddawood\_eng@uodiyala.edu.iq

Department of Mechanical Engineering, College of Engineering,  
University of Diyala, Baqubah 32001, Iraq



converted to acoustic (sound-wave) power and vice versa [4]. Thermoacoustic devices can be classified into two main categories: engines and refrigerators. Refrigerators convert sound energy into heat energy (create cooling effect), whereas engines turn thermal energy into sound energy, which may then be utilized to generate electrical energy through the loudspeaker. Thermoacoustic devices have two modes of operation: standing-wave and traveling-wave. Standing-wave thermoacoustic devices are less expensive and simpler to manufacture (compared to traveling-wave thermoacoustic devices) with less thermal performance [6].

Sound waves can be generated using either a thermoacoustic engine or an acoustic power generator (ordinary loudspeaker or liner alternator). Thermoacoustic refrigerators use sound waves to pump heat from the cooling space (low temperature) to the surrounding environment (high temperature). The main components of a standing-wave thermoacoustic refrigerator are the acoustic driver (loudspeaker), a resonator usually a tube filled with the operating gas (helium, air, etc.). In addition, a porous stack consisting of several parallel plates is placed inside the resonator and two heat exchangers are placed on both sides of the stack (ambient and cold). The sound wave from the acoustic driver causes the gas parcels to oscillate back and forth in the direction of wave propagation. The acoustic standing wave compresses and expands the gas, causing a temperature difference along the stack. A cooling effect occurs when there is thermal contact between the solid boundaries of the stack and the gas parcels. A detailed explanation of the operating principles of thermoacoustic refrigerators is given by Swift [7].

The thermoacoustic phenomenon was introduced, theoretically developed, and explained by Rott, in 1980 [8]. This paved the path for many researchers helping them in the process of construction of thermoacoustic devices, as Hofler [9] produced the first standing-wave thermoacoustic refrigerator. This refrigerator was supplied with an acoustic driver to run at an operating frequency of 500 Hz and its working gas was helium at 10 bars. A heat/cooling load of 3 W was applied to achieve an efficiency of up to 12% relative to Carnot. Adeff and Hofler [10] have successfully built and tested a thermoacoustic refrigerator driven by solar energy. Their refrigerator was capable of reaching 2.5W of cooling power at a lowest temperature of 5 °C, making cooling possible in remote areas. Wetzler and Herman [11] have developed a thermoacoustic refrigerator design algorithm. The proposed algorithm can be used as a simple design guide for thermoacoustic refrigerators. Tijani et al. [12] used their algorithm to design and build a thermoacoustic refrigerator. The researchers also focused on numerical and experimental studies of the standing-wave thermoacoustic

refrigerator to develop the properties of the stack's material, geometry, and location inside the resonator [13–19]. Kajurek et al. [20] designed a mini-fridge with a cooling power of 10 W and a temperature difference of 30 °C. The numerical special tool DELTAEC (Design for Low Amplitude Thermoacoustic Energy Conversion) was used to simulate their design. The simulation was performed at different temperatures for the cold heat exchanger and different driving ratios. According to the simulation results, the cooling power of the refrigerator increases as the drive ratio and the temperature of the cold heat exchanger increase. Prashantha [21] has also made a contribution by providing a special strategy for improving the design of thermoacoustic refrigerators. Prashantha provided a guide for other thermoacoustic researchers by designing and developing thermoacoustic refrigerators, using helium and air as working gases. The results showed that helium is superior to air in terms of cooling capacity. His theoretical results were compared with the DELTAEC simulation showing very good matching with each other.

Based on the authors' knowledge of the prior literature, it is clear that the cooling power and performance of standing-wave thermoacoustic refrigerator is still relatively low. Therefore, the novelty of this study is that it designs a standing-wave thermoacoustic refrigerator driven by an ordinary loudspeaker at a low cost. This refrigerator is able to achieve high cooling power and raise the coefficient of performance (COP) of thermoacoustic refrigerator and can compete with conventional refrigeration systems. In addition, conducted a study on the effect of parameters on cooling power and thermal/overall performance using the DELTAEC program. This cooling technology has many advantages, some of which have already been introduced, including being a great renewable technology (using solar energy or the waste heat of a combustion engine or power plant as a heat source to drive a thermoacoustic heat engine, producing acoustic energy for thermoacoustic refrigerators), being environmentally friendly and maintenance free.

### 1.1 Electroacoustic power transducer

Thermoacoustic refrigerators require an acoustic driver for generating sound waves and creating a cooling effect. The electroacoustic transducer converts electrical power into acoustic power or vice versa. Many transducer mechanisms can be used. The most common is electrodynamics. An ordinary loudspeaker and a linear alternator are electrodynamic transducer mechanisms. Ordinary loudspeakers are readily available, relatively low-cost, and can be used in relatively low power thermoacoustic applications. They produce relatively low sound power due to their fragile paper

cone and limited stroke lengths. In general, the efficiency of ordinary loudspeakers is relatively low compared to linear alternators. However, linear alternators are more expensive due to the lack of research and manufacturers. Linear alternators are used in high-power thermoacoustic applications [4, 22, 23]. Hence, an ordinary loudspeaker (model: xm004\_04) was chosen for the present design of a thermoacoustic refrigerator for the reasons of it is low cost and commercial availability (see Table 1).

For a good coupling, the resonance frequency of the acoustic driver should equal the working frequency of the thermoacoustic refrigerator. The performance of the acoustic driver depends on the acoustic conditions of the thermoacoustic refrigerator, which are represented by the acoustic impedance and its phase. In other words, it is necessary to match the acoustic impedance of the acoustic driver and refrigerator. Acoustic impedance is the ratio between the difference in pressure on both sides of the piston (the diaphragm) and the volumetric flow ratio ( $|Z_a| = \frac{|\Delta P|}{|U|}$ ) and its phase ( $\theta_{Z_a} = \theta_{\Delta p} - \theta_U$ ) [4, 25].

The acoustic power output of the acoustic driver can be calculated from Eq. (1).

$$\dot{E}_{AD} = \frac{1}{2} |\Delta P| |U| \cos \theta_{(Z_a)} \quad (1)$$

Similarly, the electrical power consumed by the acoustic driver can be easily obtained from Eq. (2).

$$\dot{W}_{AD} = \frac{1}{2} |I| |V| \cos \theta_{(I,V)} \quad (2)$$

The acoustic driver performance (efficiency) is equal to the acoustic power produced by the electrical power consumed. It can be expressed by Eq. (3).

$$\eta_{AD} = \frac{\dot{E}_{AD}}{\dot{W}_{AD}} \quad (3)$$

As we explained previously, obtaining the maximum acoustic power and high efficiency depends on the acoustic conditions. In other words, an appropriate acoustic impedance amplitude and phase must be provided on both sides of the diaphragm. An analysis was carried out on the loudspeaker (model: xm004\_04), and Fig. 1 shows the acoustic power produced, the electrical power consumed, and efficiency using each of the (1, 2, 3) equations. Using the cross-diaphragm acoustic impedance (70 to 95 Kpa.s/m<sup>3</sup>) and its phase between 90 ° and –90 ° (the phase of the volumetric flow rate leads or lags the phase of a pressure difference by 90 ° to –90 °), with an operating frequency and peak-to-peak diaphragm displacement of 110 Hz and 7 mm, respectively. It can be noted that the maximum efficiency of loudspeaker and acoustic power is achieved at around 100 watts at acoustic impedances ranging (from 70 to 95 Kpa.s/m<sup>3</sup>) and phases ranging (from –70° to –85 °), as shown in Fig. 1.

## 2 Design methodology of the standing-wave thermoacoustic refrigerator

The DELTAEC simulation program was utilized to design the standing-wave thermoacoustic refrigerator. In the previous section, it was shown that the optimum efficiency and power of the given ordinary loudspeaker can be easily achieved after meeting the appropriate acoustic conditions. Consequently, the next step was to design the standing-wave thermoacoustic refrigerator around the targeted acoustic conditions with an operating frequency, mean pressure, and temperature differential between ambient and cold heat exchangers (AHX and CHX) of 110 Hz, 1 bar, and 25 K, respectively. In the DELTAEC simulation, the pressure amplitude, the mean temperature, the phase pressure amplitude, the heat removed from the hot heat exchanger, and the cooling load applied to the cold heat exchanger were set as the guess parameters. The real and imaginary parts of the inverse of the normalized acoustic impedance and the total energy flow determined at the final segment of the device were set as the target parameters, with the temperature of the hot and cold heat exchangers at 300 K and 275 K, respectively, as shown Fig. (2).

### 2.1 3.1 The working gas

The choice of working gas has a significant impact on the performance of the thermoacoustic devices. However, in order to choose the appropriate working gas of the thermoacoustic refrigerator, there are several characteristics to consider, such as Prandtl number, sound velocity, thermal conductivity, and viscosity. It's worth noting

**Table 1** The main parameters of the ordinary loudspeaker [24]

Parameter	Value
Effective area <b>A</b> (cm <sup>2</sup> )	342
Electrical resistance <b>Re</b> (Ω)	3.5
Mechanical resistance <b>Rm</b> (N.s/m)	6.53
Coil inductance <b>L</b> (mH)	2.3
Moving mass <b>M</b> (kg)	0.16
Force factor <b>Bl</b> (N/A)	17.7
Spring constant <b>K</b> (N/m)	4166.667
Frequency range <b>f</b> (Hz)	20–1000
Maximum voltage <b> V </b> (volts)	44.7
Maximum current <b> I </b> (amps)	6.8
Maximum peak-to-peak diaphragm's displacement <b> 2ξ </b> (mm)	30

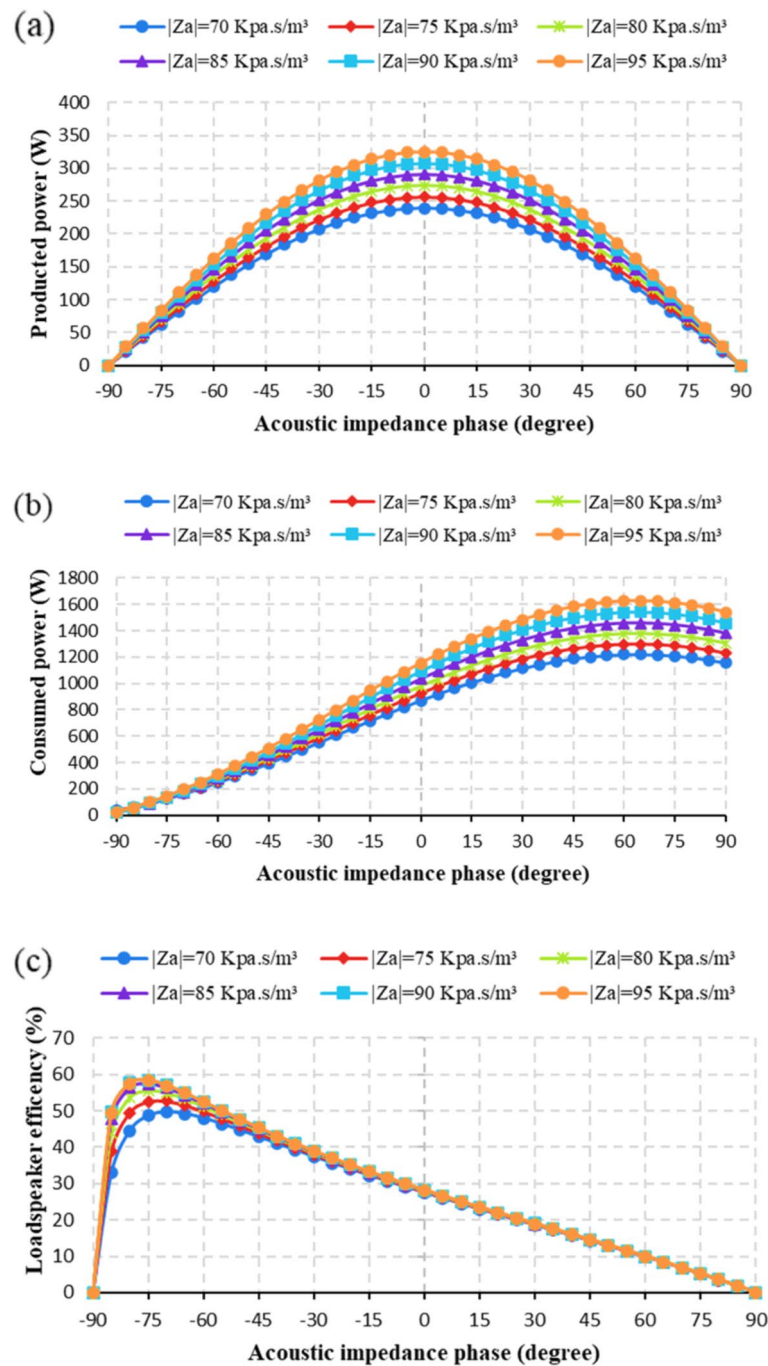


**Fig. 1** Acoustic power produced (a), the electrical power consumed (b), and efficiency (c) of the ordinary loudspeaker

that a low Prandtl number means less viscous dissipation, whereas a high thermal conductivity means more thermal penetration depth. Hence, larger gaps of the stack and heat exchangers (easier to build) are not always the right choice to consider. For the present design, helium was used as the working gas due to the advantages of wide availability, low cost, low Prandtl number, high

speed of sound, and thermal conductivity [4, 26, 27]. Table 2 shows the properties of helium gas at 110 Hz.

### 2.2 3.2 Thermoacoustic refrigerator device

Thermoacoustic refrigerator consists of several components. Figure 2 shows a schematic diagram of the

**Table 2** Characteristics of helium gas

Prandtl number	0.67889
Sound velocity	1027.8 m/s
Thermal conductivity	0.15429 W/(m.K)

standing-wave thermoacoustic refrigerator and its components.

**2.2.1 The loudspeaker and its house**

The loudspeaker is used to convert electric power to acoustic power (excitation of acoustic waves), which is needed by the thermoacoustic refrigerator, as explained in Sect. 2. Thus, the loudspeaker was located inside a box (driver’s house) which works to equalize the pressure on both sides of the diaphragm to prevent damage during the charging process.

**2.2.2 Thermoacoustic core**

The thermoacoustic core consists of two important parts: the stack and two heat exchangers (AHX and CHX). The stack (where the thermoacoustic effect occurs) can be considered as the most important component of the standing-wave thermoacoustic refrigerator. Small changes in its dimensions may result in large changes in the thermal performance of the refrigerator. It is usually made of a material with low thermal conductivity to avoid losing a lot of acoustic power. In addition, it should have a heat capacity greater than the working gas’s heat

capacity [28]. In the current model, Mylar was chosen for its low conductivity. The stack could be made with different geometries, such as parallel plates, circular holes, pin arrays, and triangular pores. However, some of them might be difficult to build. As a result, the parallel plate geometry was chosen as the stack for the present design and to be fabricated later. On the other hand, the space between the working gas parcel and the solid surfaces of the plate is an important factor during stack design to be considered concerning the approach of the heat transfer process. The thermal and viscous penetration depths are important parameters in determining the spacing between the plates of the stack, through which the heat transfer and effect of viscosity between the plate and working gas parcel can be estimated, see Eqs. (4) and (5).

$$\delta_k = \sqrt{\frac{2k}{\omega\rho C_p}} \tag{4}$$

$$\delta_v = \sqrt{\frac{2\mu}{\omega\rho}} \tag{5}$$

The ambient and cold heat exchangers (located at the ends of the stack) are necessary to transfer certain amounts of heat and maintain the required temperature gradient across the stack to complete the thermoacoustic cooling process. Accomplishing a proper design of these heat exchangers could be a challenging task as the flow is oscillating under the thermoacoustic effect. Preferably,

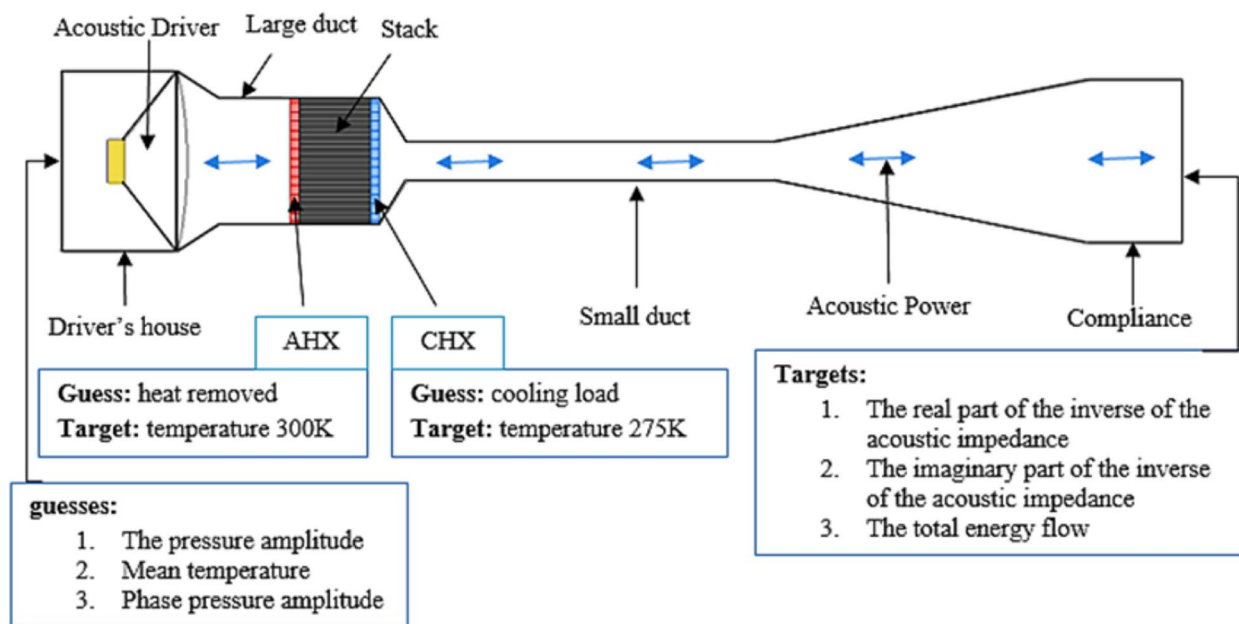


**Fig. 2** Schematic of a standing-wave thermoacoustic refrigerator driven by an ordinary loudspeaker



the cross-sectional areas of both heat exchangers and stack are to be exactly matched. In addition, the optimum heat exchanger length should be equal to the local peak-to-peak gas displacement. The gas displacement amplitude can be expressed by Eq. (6) [7].

$$|\xi| = \frac{|U|}{\omega A} \tag{6}$$

Both heat exchangers and stack represent the standing-wave thermoacoustic refrigerator’s core. This thermoacoustic core is to be placed inside a resonator for maintaining the thermoacoustic effect. The ambient heat exchanger must be located near the pressure amplitude anti-node (where the pressure is maximum) and the volume flow rate amplitude node (minimum volumetric flow rate). The cold heat exchanger is located on the other side of the stack where the volume flow rate amplitude is higher, and the pressure amplitude is slightly lower in comparison with the opposite side of the stack (AHX side). The phase difference between the pressure and the volume flow rate amplitudes should be near to 90°. Figure 3 shows the location of the thermoacoustic refrigerator’s core based on the distribution of the pressure and volumetric velocity amplitudes along its resonator.

### 2.2.3 The resonator

The resonator is the necessary part to maintain acoustic waves where the core of the thermoacoustic refrigerator is placed and then being filled with working gas. The length of the resonator must match the operating resonance frequency of the thermoacoustic system (usually a quarter or half wavelength), see Eq. (7).

$$\lambda = \frac{a}{f} \tag{7}$$

Acoustic energy can be affected by the resonator. Both viscosity and thermal penetration depths are responsible for the dissipation of acoustic energy [7]. These losses can be minimized by designing the standing-wave thermoacoustic refrigerator to have a quarter wavelength resonator which can only dissipate half of the energy compared to a half wavelength resonator due to the reduced internal surface area. Hofler [9] shows how to achieve this by reducing the diameter of the resonance tube behind the core (a small duct) called “inertance” (the term refers to long channels with small volume) and simulating an open end with a spherical bulb called “compliance” (which is the term describing short channels with large volume).

Here, both the inertance and the compliance are introduced into the model of the thermoacoustic refrigerator for the purpose of controlling the acoustic conditions (acoustic impedance and its phase). The acoustic impedance of the inertance can be represented by ( $Z_{aL} = \frac{|\Delta P|}{|U|}$ ) which shows the effect of pressure difference over the volume flow rate, while the compliance is ( $Z_{aC} = \frac{|P|}{|\Delta U|}$ ) which shows the opposite difference effect.

Figure 4 shows the effect of the diameter and length of the inertance on both of acoustic impedance and its phase. After examining Fig. 4, it can be said that increasing the length of the inertance has led to a decrease in the acoustic impedance while increasing its cross-sectional area (diameter) resulted in an increase in the acoustic impedance where the ordinary loudspeaker was located. In addition to inertance, compliance also has an effect on the acoustic conditions of

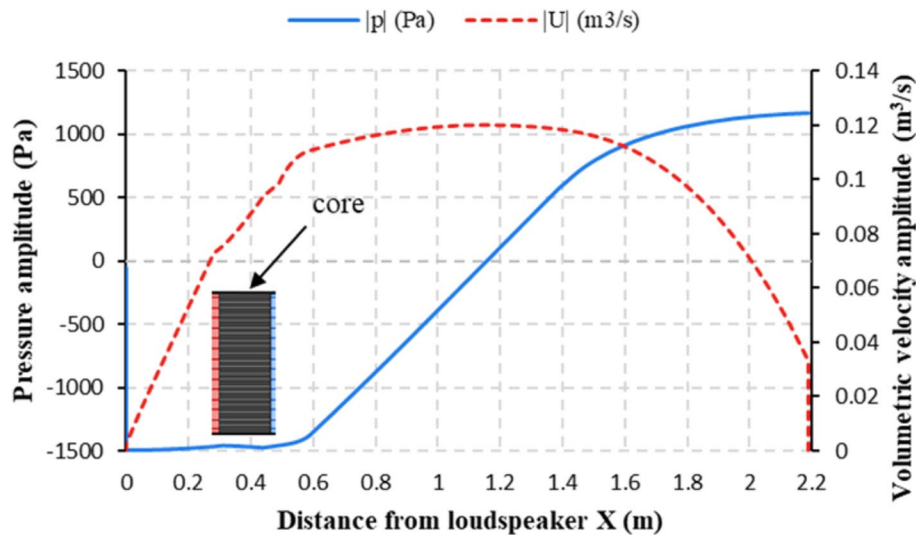


Fig. 3 Distribution of pressure amplitude, volumetric velocity amplitude, and position thermoacoustic core

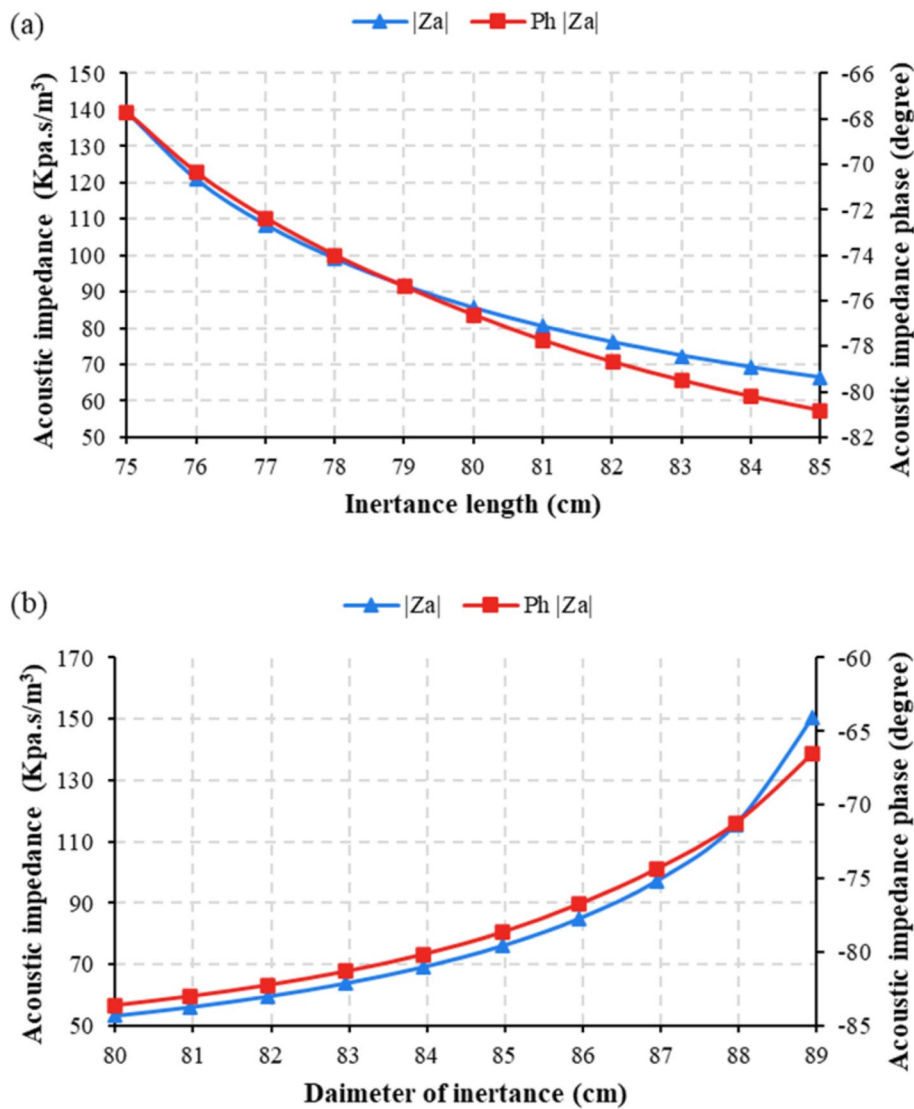


Fig. 4 The effect of inertance length (a) and diameter (b) on the acoustic impedance and its phase

the thermoacoustic system (results omitted for brevity). The utilization of both compliance and inertance provided more control of the acoustic conditions of the standing-wave thermoacoustic refrigerator.

In general, the coefficient of performance (COP) can be used to measure the thermal performance of a thermoacoustic refrigerator, which is calculated from the ratio of cooling to acoustic power, see Eq. (8).

$$COP = \frac{\dot{Q}}{E_{AD}} \tag{8}$$

However, according to the Carnot cycle, the COPC is the refrigerator's theoretical cooling capability at a given temperature difference, see Eq. (9).

$$COPC = \frac{T_c}{T_a - T_c} \tag{9}$$

Hence, the coefficient of performance relative to Carnot (COPR) is defined as the ratio of the refrigerator's COP to the COP of the Carnot cycle (COPC), see Eq. (10).

$$COPR = \frac{COP}{COPC} \tag{10}$$

The overall efficiency of the system can be calculated from the ratio of the cooling power to the electrical power consumed by the loudspeaker, see Eq. (11).

$$\eta_{overall} = \frac{\dot{Q}}{\dot{W}_{AD}} \tag{11}$$

### 3 Results and discussion

In the previous part, it was shown and discussed that the acoustic conditions necessary for the ordinary loudspeaker to perform at its best can be easily met by altering the dimensions of the resonator (especially, inertance and compliance). In this section, the effect of some parameters (cross-section, porosity, hydraulic radius, etc.) of the thermoacoustic refrigerator's core (stack and heat exchangers) on its overall efficiency, cooling power, and coefficient of performance.

#### 3.1 The effect of the thermoacoustic core location

location of the thermoacoustic core (ambient and cold heat exchangers and stack) inside the resonator can significantly affect the process of thermoacoustic cooling. Figure 5 shows the position of the thermoacoustic core (its distance from the loudspeaker – acoustic power source) in relation to the wavelength ( $X_c/\lambda$ ). Looking at Fig. 5, it can be noticed that the cooling power is maximum when the core is very close to the acoustic source and drops as it moves away from the loudspeaker. On the other hand, the values of both COP and COPR are decreasing to reach their lowest when the core is close to the acoustic source (loudspeaker). Hence, the overall efficiency of the refrigerator was also presented (see Fig. 5a) to provide the complete picture of the refrigerator's performance and being able to decide the optimum location of the core in consideration of the wavelength. Based on

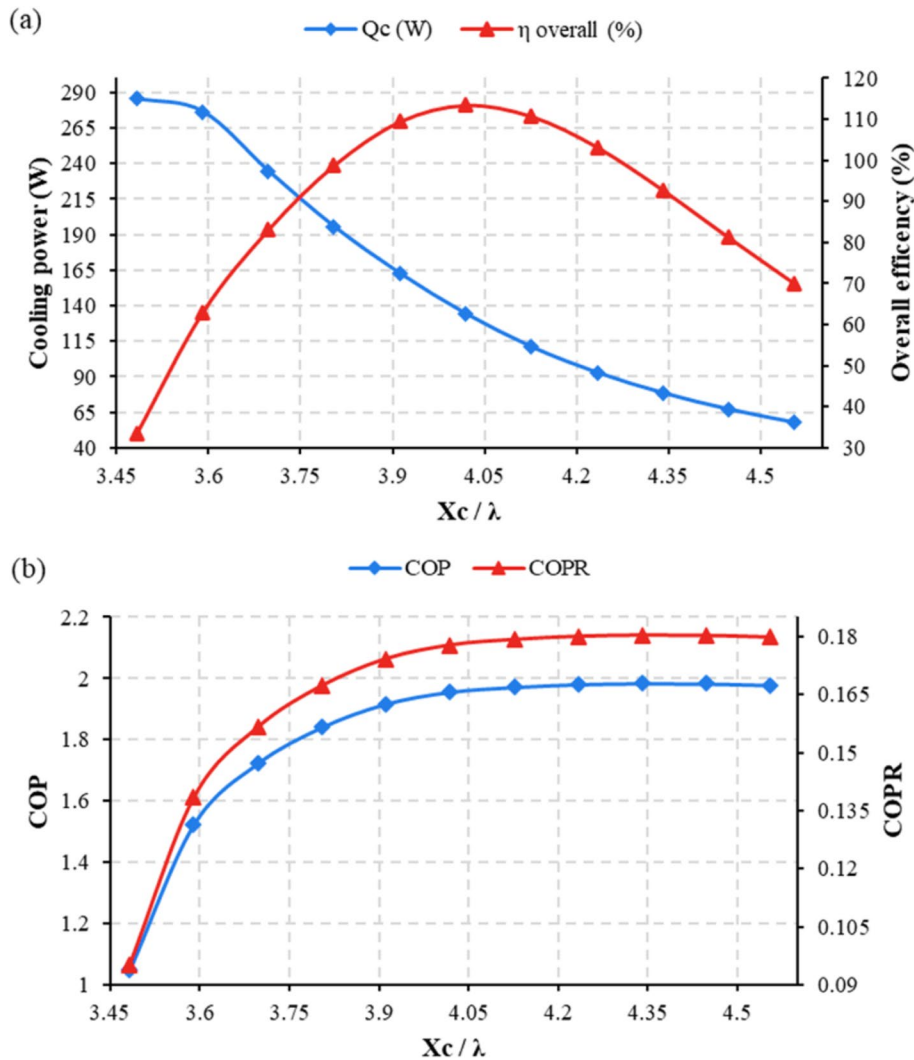


Fig. 5 The effect of the core's position to the wavelength on cooling power and overall efficiency (a) and COP and COPR (b)



the current results, it was chosen to be between 3.9 and 4.1 ( $X_c / \lambda$  — see Fig. 5a) and moved on to investigate the effect of other parameters on the thermal performance of the designed standing-wave refrigerator.

**3.2 4.2 The effect of the Lautrec number of the stack**

The dimensionless ratio between the hydraulic radius ( $r_h$ ) and the thermal penetration depth ( $\delta_k$ ) of the stack is known as the Lautrec number. The hydraulic radius is the ratio of the cross-sectional area to the perimeter of the channel (pore) of the stack. This ratio is important for the heat transfer process between the gas parcels and solid plates. Figure 6a and b shows the effect of this ratio ( $r_h/\delta_k$ ) on cooling power, overall efficiency,

and COP of the designed standing-wave refrigerator. As can be seen, both the cooling power and overall efficiency and COP and COPR will increase to a maximum value and then start to decrease. Interpretation of this, there are losses in acoustic energy as a result of viscosity when there is little spacing. Therefore, these losses decrease with the increase in spacing. On the contrary, increasing the spacing leads to weak thermal contact between the gas and the plates of the stack, which will have an impact on the heat transfer process. Here, the ratio between 1.3 and 1.5 is chosen according to the results of the data in Fig. 6a and b, and then we move to the study of another effect on the performance of the thermoacoustic refrigerator.

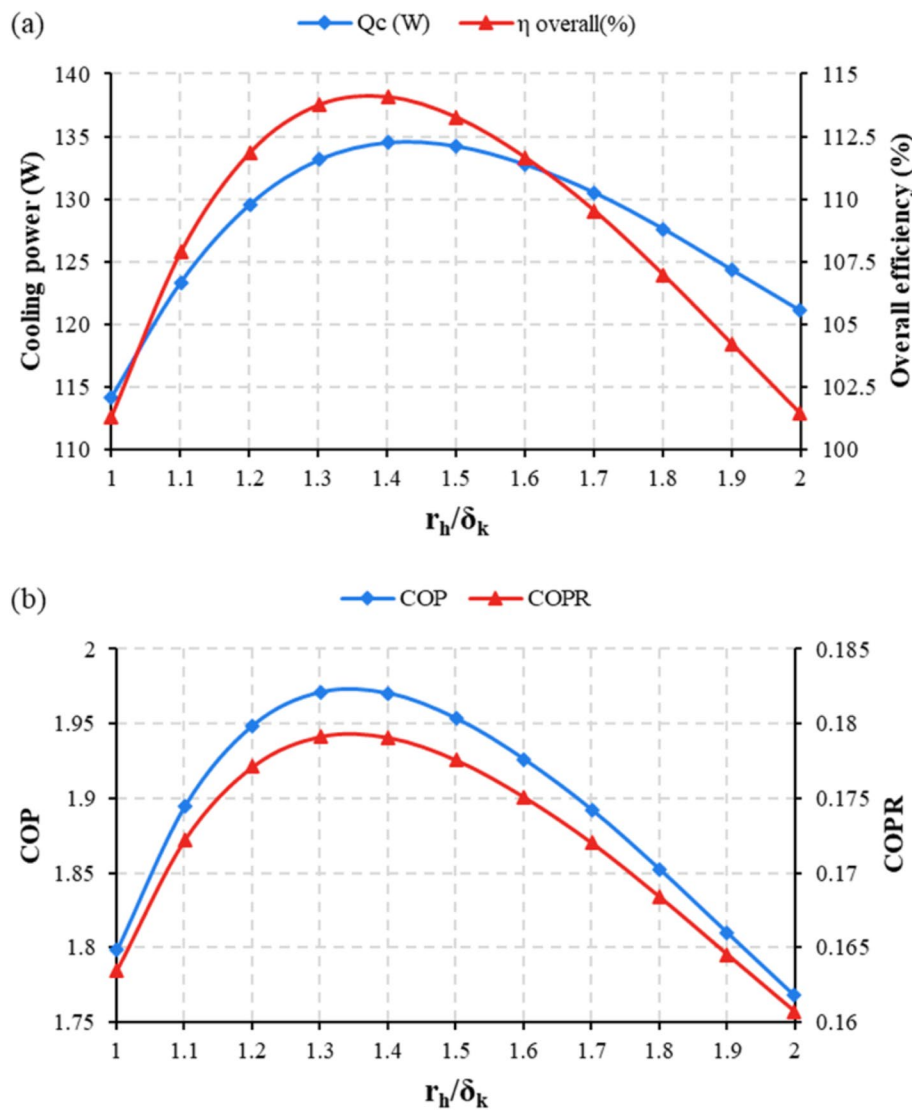


**Fig. 6** The effect of ( $r_h/\delta_k$ ) of the stack on the cooling power and overall efficiency (a) and COP and COPR (b)

### 3.3 The effect of the ratio of the diameter of the large duct to the small duct

After studying the effects of the thermoacoustic core location and the dimensionless ratio between ( $r_h$ ) and ( $\delta_k$ ) of the stack, the effect of the ratio of the large diameter to the small diameter ( $D_{large}/D_{small}$ ) has been studied on the performance of the thermoacoustic refrigerator by reducing energy losses (acoustic power dissipation as a result of viscosity and thermal losses), as shown in Fig. 7. To do this analysis, the large diameter was kept fixed and changed the small diameter. The effect of the ratio on the values of cooling power and overall efficiency can be seen in Fig. 7a, which indicates that cooling power begins to drop as the ratio increases (In general, acoustic

power can be expressed as pressure, volumetric flow rate and the phase difference between these two quantities (see Eq. 1). Therefore, in order for the loudspeaker to work at its best performance and produce the required acoustic power, it must have certain acoustic conditions, as explained in Sect. 2. However, when coupling the loudspeaker with the thermoacoustic refrigerator, the acoustic conditions of the refrigerator cannot match the acoustic conditions of the loudspeaker. Hence, there should be a way of trading between the two. These acoustic conditions around the loudspeaker and refrigerator (thermoacoustic core) are mainly controlled by compliance and inertance (a combination of small and large diameters, long and short pipes, and other volumes).

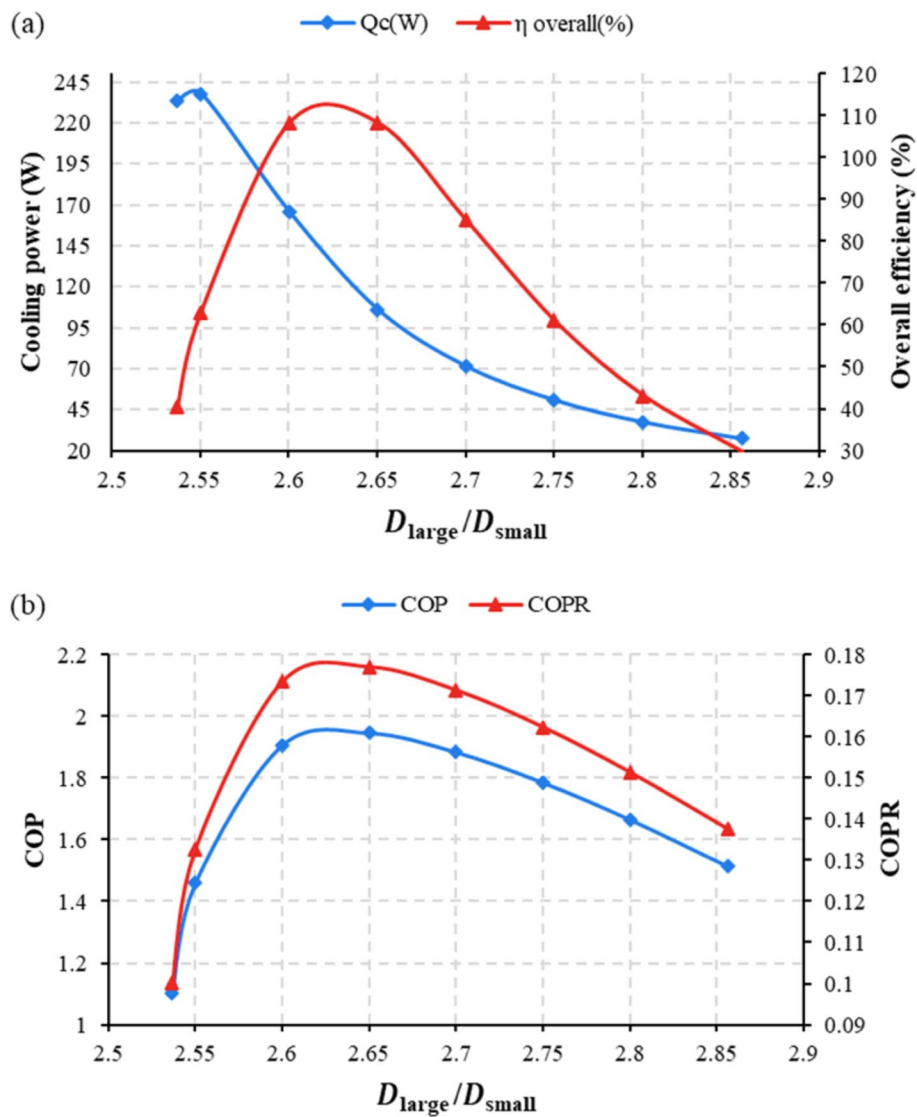


**Fig. 7** The effect of ( $D_{large}/D_{small}$ ) on cooling power and overall efficiency (a) and COP and COPR (b)

Thus, when a change in large to small diameters (see Fig. 7) is made, the acoustic conditions will meet either the requirements of the loudspeaker or thermoacoustic core. This leads to a decrease or increase of the acoustic power produced (the loudspeaker’s overall efficiency begins to increase until it reaches its maximum value and then decreases) and cooling power. In addition, both COP and COPR start increasing and then decreasing (see Fig. 7b). Accordingly, a ratio between 2.6 and 2.65 was selected to achieve the optimal cooling power and performance for the refrigerator.

### 3.4 The effect of the plate’s spacing of heat exchangers

In addition, heat exchangers have a notable impact on the thermal performance of the designed standing-wave

thermoacoustic refrigerator which is shown in Fig. 8. It shows the effect of plate spacing of the heat exchanger on the thermal/overall performance of the refrigerator. The highest performance of the thermoacoustic refrigerator is attained at a certain percentage of  $(2Y_0/\delta_k)$ , when the gas and the heat exchanger plates are in excellent thermal contact, Looking at Fig. 8a, it can be observed that the values required to achieve the appropriate cooling power are limited to a range of values between 5 and 7.5. On the other hand, when the distance between the plates increases, so do the COP and COPR values (see Fig. 8b). Based on the results shown in Fig. 8a and b, it can be chosen the value  $(2Y_0/\delta_k)$  is equal to 7, taking into account both cooling power (cooling loads) and thermal/overall performance.

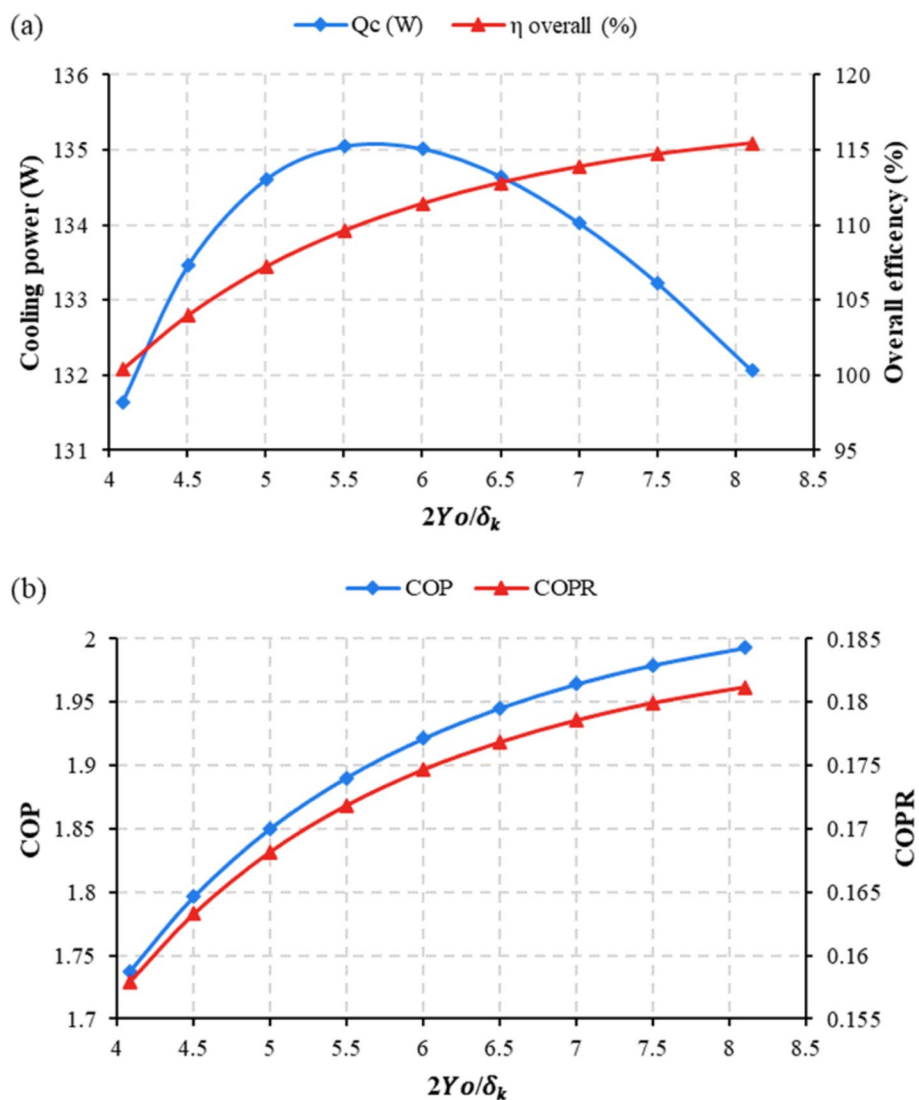


**Fig. 8** The effect of plate spacing  $(2Y_0/\delta_k)$  of heat exchanger on cooling power and overall efficiency (a) and COP and COPR (b)

**Table 3** The dimensions of the optimized design of standing-wave thermoacoustic refrigerator

Component	Diameter (mm)	Length (mm)	Hydraulic radius (mm)	Porosity (%)
Stack	225.67	130	1	83.3
Ambient heat exchanger	225.67	30	2.5	52
Cold heat exchanger	225.67	50	2.5	52
Large duct	225.67	190	-----	-----
Small duct (inertance)	86	800	-----	-----
Compliance	250	138.77	-----	-----
<b>Other optimized parameters</b>				
$Xc/\lambda = 4.019$	$r_h/\delta_k = 1.4884$		$D_{large}/D_{small} = 0.262$	$2Y_0/\delta_k = 7.44$

The final and optimized dimensions of the numerically designed standing-wave thermoacoustic refrigerator are shown in Table 3. These dimensions are chosen to achieve the maximum possible cooling power and overall efficiency after going through the results of the current investigation.

#### 4 Conclusions

In conclusion, a standing-wave thermoacoustic refrigerator was designed and simulated using the DeltaEC simulation program, driven by an ordinary loudspeaker. In addition, the ordinary loudspeaker was analyzed to determine its optimal performance by finding the appropriate acoustic conditions (acoustic impedance and its phase), as well as matching the acoustic conditions between the loudspeaker and the thermoacoustic refrigerator. However, the results obtained in locating the position of the thermoacoustic core in relation to the wavelength, as well as the ratio of large to small diameter and the ratio of the spacing between plates of the stack and heat exchangers, would be appreciated to utilize them in designing a standing-wave thermoacoustic refrigerator in the future. Thus, the optimized thermoacoustic refrigerator is capable of achieving a cooling power of 134.34 watts at a difference in temperatures on both the ambient and cold heat exchangers at 25 K. The overall efficiency was 113.43%, and the coefficient of performance (COP) was 1.956. These results could be further improved by utilizing a linear alternator (highly rated power) instead of the used ordinary acoustic driver. However, this would increase the total cost of the apparatus which has been avoided in the present design.

#### 5 Nomenclature

$\dot{E}_{AD}$  Acoustic power (W)  
 $\dot{W}_{AD}$  Electrical power (W). $\eta$ Efficiency (%)  
 $|Z_a|$  Acoustic impedance (Kpa.s/m<sup>3</sup>)  
 $|\Delta P|$  Pressure difference (Pa)

$|U|$  Volume flow rate (m<sup>3</sup>/s)  
 $|\xi|$  Displacement of gas (m)  
 $\delta_k$  Thermal penetration depth (m)  
 $\delta_v$  Viscous penetration depth  
 $k$  Thermal conductivity (W/m.K)  
 $\rho$  Density (kg/m.<sup>3</sup>)  
 $C_p$  Isobaric specific heat capacity (J/kg.K)  
 $\mu$  Dynamic viscosity (kg/m.s)  
 $r_h$  Hydraulic radius (m)  
 $2Y_0$  Plate spacing  
 AHX Ambient heat exchanger  
 CHX Cold heat exchanger  
 COP Coefficient of performance  
 COPR Coefficient of performance relative to Carnot  
 COPC Carnot coefficient of performance  
 $T_c$  Temperature of the cold reservoir (K)  
 $T_a$  Temperature of the Ambient reservoir (K)  
 $\dot{Q}$  Cooling power (W)  
 $\theta$  Phase angle (Degree)  
 $|V|$  Driver's voltage (volt)  
 $|I|$  Driver's current (amp)  
 $\lambda$  Wavelength (m)  
 $a$  Sound speed (m/s)  
 $f$  Frequency (Hz)  
 $\omega$  Angular frequency (s<sup>-1</sup>)  
 ADA Acoustic driver  
 A Area (m<sup>2</sup>)  
 $R_e$  Coil resistance ( $\Omega$ )  
 $R_m$  Electrical resistance (N.s/m)  
 L Coil inductance (mH)  
 $M$  Moving mass (Kg)  
 B I Force factor (N/A)  
 $\text{K}$  Spring constant (N/m)

#### Authors' contributions

The authors read and approved the final manuscript.

#### Availability of data and materials

The datasets generated during and/or analyzed during the current study are available from the corresponding author on reasonable request.

## Declarations

### Competing interests

The authors have no competing interests to declare that are relevant to the content of this article.

Received: 2 June 2022 Accepted: 3 March 2023

Published online: 14 March 2023

## References

- Alamir, M. A., & Sidik, N. A. C. (2021). Thermoacoustic Refrigerators and Heat Pumps: New Insights for A High Performance. *Journal of Advanced Research in Fluid Mechanics and Thermal Sciences*, 78(1), 146–156. <https://doi.org/10.37934/arfmts.78.1.146156>
- Zolpakar, N. A., Mohd-Ghazali, N., & El-Fawal, M. H. (2016). Performance analysis of the standing wave thermoacoustic refrigerator: A review. *Renewable and Sustainable Energy Reviews*, 54, 626–634. <https://doi.org/10.1016/j.rser.2015.10.018>
- Tartibu, L. K. (2016). A sustainable solution for refrigeration using thermo-acoustic technology (March 2016). *International Conference on the Domestic Use of Energy (DUE)*, 1–8. <https://doi.org/10.1109/DUE.2016.7466714>
- Keolian, R. M., Garrett, S. L., & Garrett, S. L. (2018). Thermoacoustics: A Unifying Perspective for Some Engines and Refrigerators, Second Edition. *Acoustical Society of America Journal*, 143(4), 2110–2110. <https://doi.org/10.1121/1.5031020>
- Prashantha, B. G., Govinde Gowda, M. S., Seetharamu, S., & Narasimham, G. S. V. L. (2017). Design construction and performance of 10 W thermoacoustic refrigerators. *International Journal of Air-Conditioning and Refrigeration*, 25(03), 1750023. <https://doi.org/10.1142/S2010132517500237>
- Mahmood, O. S., Karim, A. M. A., Yahya, S. G., & Azzawi, I. D. J. (2020). Miniaturized Traveling-Wave Thermoacoustic Refrigerator Driven by Loudspeaker: Numerical Design. *International Journal of Air-Conditioning and Refrigeration*, 28(04), 2050035. <https://doi.org/10.1142/S2010132520500352>
- Swift, G. W. (1988). Thermoacoustic engines. *The Journal of the Acoustical Society of America*, 84(4), 1145–1180. <https://doi.org/10.1121/1.396617>
- Rott, N. (1980). Thermoacoustics. *Advances in Applied Mechanics*, 20, 135–175. [https://doi.org/10.1016/S0065-2156\(08\)70233-3](https://doi.org/10.1016/S0065-2156(08)70233-3)
- Hofler, T. J. (1986). Thermoacoustic Refrigerator Design and Performance (Heat Engine, Resonator, Microphone). PhD thesis, University of California, San Diego. <https://www.proquest.com/openview/46e288d402bfc5f48cb23c693bbb17b9/1?pqorigsite=gscholar&cb=18750&diss=y>
- Adeff, J. A., & Hofler, T. J. (2000). Design and construction of a solar-powered, thermoacoustically driven, thermoacoustic refrigerator. *The Journal of the Acoustical Society of America*, 107(6), L37–L42. <https://doi.org/10.1121/1.429324>
- Wetzel, M., & Herman, C. (1997). Design optimization of thermoacoustic refrigerators. *International Journal of Refrigeration*, 20(1), 3–21. [https://doi.org/10.1016/S0140-7007\(96\)00064-3](https://doi.org/10.1016/S0140-7007(96)00064-3)
- Tijani, M. E. H., Zeegers, J. C. H., & De Waele, A. T. A. M. (2002). Construction and performance of a thermoacoustic refrigerator. *Cryogenics*, 42(1), 59–66. [https://doi.org/10.1016/S0011-2275\(01\)00180-1](https://doi.org/10.1016/S0011-2275(01)00180-1)
- Alamir, M. A. (2019). Experimental study of the stack geometric parameters effect on the resonance frequency of a standing wave thermoacoustic refrigerator. *International Journal of Green Energy*, 16(8), 639–651. <https://doi.org/10.1080/15435075.2019.1602533>
- Zolpakar, N. A., & Mohd-Ghazali, N. (2019). Comparison of a thermoacoustic refrigerator stack performance: Mylar spiral, celcor substrates and 3D printed stacks. *International Journal of Air-Conditioning and Refrigeration*, 27(03), 1950021. <https://doi.org/10.1142/S2010132519500214>
- Yahya, S. G., Mao, X., & Jaworski, A. J. (2017). Experimental investigation of thermal performance of random stack materials for use in standing wave thermoacoustic refrigerators. *International journal of refrigeration*, 75, 52–63. <https://doi.org/10.1016/j.jirefrig.2017.01.013>
- Tijani, M. E. H., Zeegers, J. C. H., & De Waele, A. (2002). The optimal stack spacing for thermoacoustic refrigeration. *The Journal of the Acoustical Society of America*, 112(1), 128–133. <https://doi.org/10.1121/1.1487842>
- Alcock, A. C., Tartibu, L. K., & Jen, T. C. (2017). Experimental investigation of ceramic substrates in standing wave thermoacoustic refrigerator. *Procedia Manufacturing*, 7, 79–85. <https://doi.org/10.1016/j.promfg.2016.12.021>
- Atiqah Zolpakar, N., Mohd-Ghazali, N., & Ahmad, R. (2017). Optimization of the stack unit in a thermoacoustic refrigerator. *Heat Transfer Engineering*, 38(4), 431–437. <https://doi.org/10.1080/01457632.2016.1195138>
- Tartibu, L. K. (2016). Maximum cooling and maximum efficiency of thermoacoustic refrigerators. *Heat and Mass Transfer*, 52(1), 95–102. <https://doi.org/10.1007/s00231-015-1599-y>
- Kajurek, J., Rusowicz, A., & Grzebielec, A. (2019). Design and simulation of a small capacity thermoacoustic refrigerator. *SN Applied Sciences*, 1(6), 1–9. <https://doi.org/10.1007/s42452-019-0569-2>
- Prashantha, B. G., Swamy, D. R., Soragaon, B., & Nanjundeswaraswamy, T. S. (2020). Design optimization and analysis of thermoacoustic refrigerators. *Int. J. Air-Conditioning Refrig.*, 28(3), 2050020. <https://doi.org/10.1142/S2010132520500200>
- Timmer, M. A., de Blok, K., & van der Meer, T. H. (2018). Review on the conversion of thermoacoustic power into electricity. *The Journal of the Acoustical Society of America*, 143(2), 841–857. <https://doi.org/10.1121/1.5023395>
- Yu, Z., Saechan, P., & Jaworski, A. J. (2011). A method of characterising performance of audio loudspeakers for linear alternator applications in low-cost thermoacoustic electricity generators. *Applied acoustics*, 72(5), 260–267. <https://doi.org/10.1016/j.apacoust.2010.11.011>
- "SEAS: The Art Of Sound Perfection." <http://www.seas.no/> (accessed 28 Apr. 2022).
- Yahya, S. G., Azzawi, I. D., Abbas, M. K., & Al-Rubaiy, A. A. (2019). Characteristics of acoustic drivers for efficient coupling to thermoacoustic machines. *Proc. of the Int. MultiConference of Engineers and Computer Scientists*, Hong Kong, IMECS 2019, 469–474. [http://www.iaeng.org/publication/IMECS2019/IMECS2019\\_pp469-474.pdf](http://www.iaeng.org/publication/IMECS2019/IMECS2019_pp469-474.pdf)
- Tijani, M. E. H., Zeegers, J. C. H., & De Waele, A. T. A. M. (2002). Design of thermoacoustic refrigerators. *Cryogenics*, 42(1), 49–57. [https://doi.org/10.1016/S0011-2275\(01\)00179-5](https://doi.org/10.1016/S0011-2275(01)00179-5)
- Ke, H., He, Y., Liu, Y., & Cui, F. (2012). Mixture working gases in thermoacoustic engines for different applications. *International Journal of Thermophysics*, 33(7), 1143–1163. <https://doi.org/10.1007/s10765-012-1268-z>
- Bouramdane, Z., Bah, A., Alaoui, M., & Martaj, N. (2022). Numerical analysis of thermoacoustically driven thermoacoustic refrigerator with a stack of parallel plates having corrugated surfaces. *International Journal of Air-Conditioning and Refrigeration*, 30(1), 1–19. <https://doi.org/10.1007/s44189-022-00002-8>

## Publisher's Note

Springer Nature remains neutral with regard to jurisdictional claims in published maps and institutional affiliations.